

## Review

Esteban Pedrueza-Villalmanzo, Francesco Pineider and Alexandre Dmitriev\*

# Perspective: plasmon antennas for nanoscale chiral chemistry

<https://doi.org/10.1515/nanoph-2019-0430>

Received October 17, 2019; revised January 12, 2020; accepted January 14, 2020

**Abstract:** Plasmon nanoantennas are extensively used with molecular systems for chemical and biological ultra-sensing, for boosting the molecular emissive and energy transfer properties, for nanoscale catalysis, and for building advanced hybrid nanoarchitectures. In this perspective, we focus on the latest developments of using plasmon nanoantennas for nanoscale chiral chemistry and for advancing molecular magnetism. We overview the decisive role nanoplasmonics and nano-optics can play in achieving chirally selective molecular synthesis and separation and the way such processes might be precisely controlled by potentially merging chirality and magnetism at the molecular scale. We give our view on how these insights might lead to the emergence of exciting new fundamental concepts in nanoscale materials science.

**Keywords:** nanoantennas; plasmonics; chirality; asymmetric reactions.

Chirality, or structural handedness, is a fundamental feature of biological life. It refers to chemically identical molecular species having non-superimposable structural arrangements. It is then said that such molecular species have one or the other handedness. This lends an extremely high specificity to a host of different molecular interactions and to build complex molecular architectures that are the fundamental building blocks in life science, biomedicine, and the pharmacological industry. Asymmetric chemical synthesis caters to these extensive needs and is employed to produce molecular species with

designed handedness, that is, an enantiomeric excess in the final product of a chemical reaction. Various catalysts are used to promote enantiomeric excess, typically in the same (liquid) phase as the reactants (homogeneous asymmetric catalysis). This usually complicates the task of separating the products from the catalyst after the reaction. Heterogeneous (surface-based) catalysis then comes to help [1]. A convenient way of measuring the enantiomeric excess and, in general, molecular chirality is by detecting the preferential absorption of right- or left-circularly polarized (RCP or LCP) light that passes through the liquid sample. Such preferential absorption is expressed as circular dichroism (CD):  $CD \propto A_{RCP} - A_{LCP}$ . Another parameter that is often employed to characterize molecular chirality is the Kuhn dissymmetry factor  $g$ , also expressed through circular polarization-dependent light absorption as  $g = \frac{2(A_{RCP} - A_{LCP})}{A_{RCP} + A_{LCP}}$ . However,  $g$  values

are typically small and, more in general, CD signals are low in dilute solutions. As a consequence, extensive research efforts are directed both at generally increasing the enantiomeric excess of the products of the asymmetric synthesis and at substantially boosting the detection sensitivity of the chiral molecular species. The latter is widely featured in the recent literature [2–4], so in this perspective we focus on the former, that is, several recent advances and future prospects of driving chiral chemistry at the nanoscale aimed at achieving sizeable enantiomeric excess. Figure 1 summarizes the discussion that follows: we overview four different paths for producing enantiomeric excess with nano-confined asymmetric chemical reactions, namely employing superchiral electromagnetic fields in plasmon cavities, Fano-type resonances, propagating surface plasmon polaritons and chiral-induced electronic spin selectivity.

CD spectroscopy is a staple spectroscopic technique to detect and quantify enantiomeric excess. Interestingly, it has been demonstrated that the use of circularly polarized (CP) light of either handedness in photochemical reactions can in itself promote the formation of one enantiomer over the other simply by the selective absorption of light with different handedness [5, 6]. Unfortunately

\*Corresponding author: Alexandre Dmitriev, Department of Physics, University of Gothenburg, Göteborg, Sweden, e-mail: alexd@physics.gu.se. <https://orcid.org/0000-0002-2231-9333>

Esteban Pedrueza-Villalmanzo: Department of Physics, University of Gothenburg, Göteborg, Sweden

Francesco Pineider: Department of Chemistry and Industrial Chemistry and INSTM, University of Pisa, Pisa, Italy

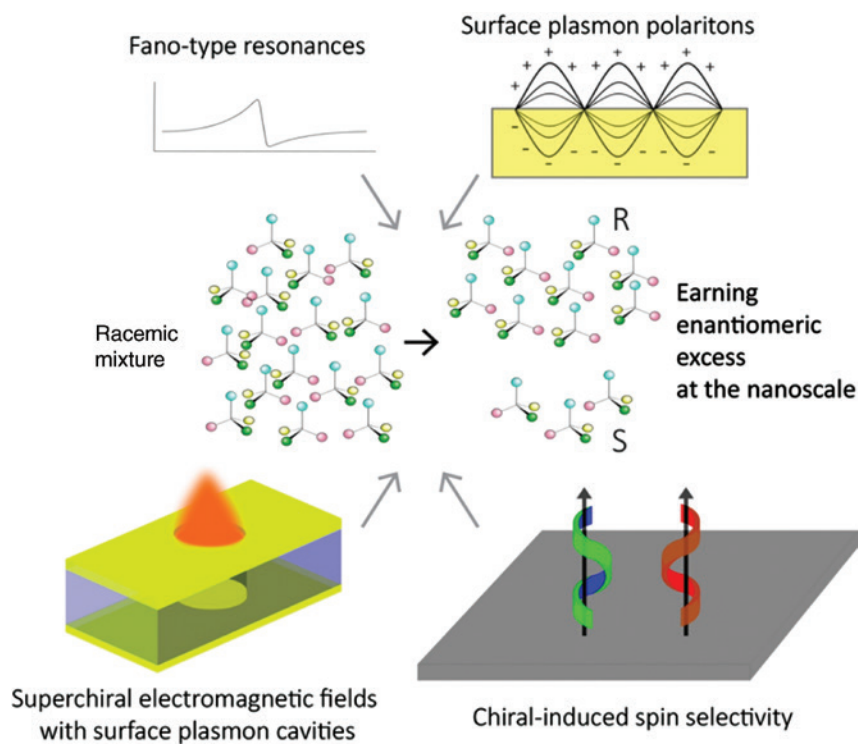


**Figure 1:** Nanoscale chiral chemistry.

Producing enantiomeric excess with nano-confined asymmetric chemical reactions (i.e. going from a racemic mixture to the strong preference of one enantiomer in the mix – see the center schematics) could be accomplished in several ways. Many of these involve confining light to the nanoscale with the nanoplasmons. Upper right: Propagating surface plasmon polaritons (SPPs) are the collective and coherent oscillation of the free electrons at a metal-dielectric interface. Producing strongly enhanced (evanescent) optical near-field, SPPs also exert circular light-polarization-dependent lateral optical forces onto a dielectric medium, helping to physically separate chiral media with the opposite structural handedness. Upper left: In nanoplasmonics, Fano-type resonances are generally produced by the interaction of two or more electromagnetic modes in a single nanoplasmon antenna or a collection of them. Such interaction often leads to highly asymmetric optical resonance line shapes, with associated sizeable optical nonlinearities and the presence of strongly confined electromagnetic fields. Lower left: Specially shaped nanoplasmonic antennas (like a nanohole in metal film against a metallic mirror) form so-called plasmonic cavities, where “superchiral” (i.e. chiral electromagnetic fields much stronger than those associated with free-space propagating circularly polarized light) near-fields emerge upon illumination with the circularly polarized light. Lower right: With chiral-induced spin selectivity (CISS), electron transport through the chiral molecules depends on the electronic spin. This effect can be employed with magnetic surfaces to separate molecular enantiomers.

though, as it is pointed out in [7], the actual chiral selectivity and the yield of such reactions are rather low, around 2%. In Figure 2A, it is possible to appreciate the small signature on the CD measurement (less than 1 mdeg) which represents an enantiomeric excess of 0.4% [8]. One interesting example of the generation of CP light-induced chirality with the addition of a second irradiation by CP ultraviolet light to lock the obtained configuration is shown in Figure 2B [9].

Recent advances in the asymmetric (photo)synthesis and chiral amplification, that is, total photoconversion of a racemic mixture into one pure enantiomer, are reviewed in [10]. Among the notable implementations are the CP light-triggered asymmetric autocatalysis reactions, showing great potential in achieving nearly

enantiomerically pure solutions [11–13]. Another method of separating the enantiomers is by using optofluidics. The group of Brasselet [14, 15] developed a system of sorting chiral micrometer-size droplets depending on their handedness and using counterpropagating beams with RCP and LCP light. This approach is used to sort smaller objects as well by using the droplets as “conveyors” and employing appropriate surface functionalization discriminating between chiral and non-chiral objects (molecules or particles). A similar approach using a single laser beam was proposed based on the optical forces exerted by light in structurally chiral particles, such as carbon nanotubes [16] or cholesteric droplets [17]. Optical trapping has also been successfully employed to sort or isolate microparticles in relation to their structural

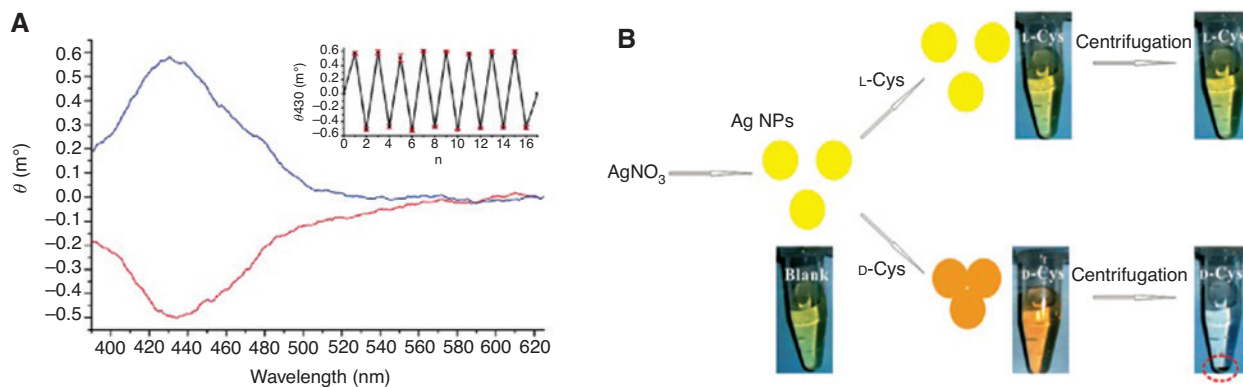


**Figure 2:** Enantiomeric excess dynamically-induced by CP light irradiation and by colorimetric discrimination using metallic nanoparticles.

(A) CD spectra ( $\theta$ ) of a photoswitchable molecule upon irradiation with RCP light (blue) and LCP light (red) at 436 nm. Inset: CD intensity values measured at 430 nm upon alternating RCP and LCP light ( $n=1-16$ ) and unpolarized light ( $n=17$ ), with standard error of mean values from three independent experiments (reproduced from Ref. [8]) – Published by The Royal Society of Chemistry. (B) Capped Ag nanoparticles (AgNPs) can be used as enantioselectors and chiral detectors platforms for D- and L-cysteine. The aggregation of AgNPs is selectively induced by an enantiomer of cysteine, which allowed the rapid colorimetric enantiodiscrimination of cysteine and separation by centrifugation. Adapted with permission from Ref. [24]. Copyright 2011 American Chemical Society.

chirality [18–20]. In a recent paper, also from the Braselot group, the role of lateral forces was used to understand a Newtonian Stern-Gerlach experiment, where a laser beam with spatially varying helicity gradient was used to displace microparticles in opposite directions depending on their handedness [21].

A promising approach to separate enantiomers in solution is the use of metal nanoparticles. While several methods rely on the use of Au [22, 23] and Ag nanoparticles [24–26], see Figure 2B these do not involve plasmon resonances, but rather the functionalization of the metallic surface with chiral or non-chiral ligands [22, 24]. Also, it has been explored the use of the colorimetric changes in Au or Ag clusters of nanoparticles [23, 25, 26] (note a helpful review in [27] on the subject).

Considering the encouraging results demonstrated by CP light-driven emergence of the enantiomeric excess in asymmetric synthesis, it is only natural to take advantage of the intense light-matter interaction at the nanoscale afforded by the plasmon resonances of metallic nanostructures in solutions or in metasurfaces. Molecular species can be found in very close contact with such nanostructures without forming a chemical bond and taking advantage of the highly enhanced electromagnetic (super) chiral near-fields in direct proximity to plasmon chiral or achiral resonators (nanoantennas). Several works have approached this exciting prospect from a theoretical point of view, yet no experimental evidence of plasmon-enhanced photochemical asymmetric synthesis has been reported so far.

Superchiral electromagnetic near-fields (i.e. electromagnetic fields with optical chirality higher than that of free-propagating CP light) can be induced in the direct proximity of the nanostructures, interacting with CP or even linearly polarized light. Such nanostructures may form extended arrays as photonic (semiconductor), plasmonic (nanometallic), or dielectric metasurfaces. The striking characteristic of these metasurfaces is that they often feature an achiral motif. We can calculate the chiral density of an electromagnetic field,  $C$ , using the following definition [28–30]:

$$C\{\mathbf{E}, \mathbf{H}\} = \frac{-k_0}{2c_0} \text{Im}\{\mathbf{E}^* \cdot \mathbf{H}\} = \frac{-k_0}{2c_0} |\mathbf{E}||\mathbf{H}| \cos(\beta_{\mathbf{E},\mathbf{H}}) \quad (1)$$

where  $\mathbf{E}$  and  $\mathbf{H}$  are the electric and magnetic fields of light;  $k_0$  and  $c_0$  are the wavevector and the speed of light in free space, respectively; and  $\beta_{\mathbf{E},\mathbf{H}}$  is the phase angle between  $i\mathbf{E}$  and  $\mathbf{H}$ . Following the calculations and assumptions on a chiral molecule described in [30], we arrive at the enhancement of the Kuhn's dissymmetry factor of the chiral molecule, relative to the one corresponding to the CPL only,  $g_{\text{CPL}}$ :

$$\frac{g}{g_{\text{CPL}}} = -\frac{1}{\omega C} \frac{|\mathbf{E}||\mathbf{H}| \cos(\beta_{\mathbf{E},\mathbf{H}})}{|\mathbf{E}|^2} \quad (2)$$

where  $\omega$  is the angular frequency of light. The main idea behind the electromagnetic design of a nanoantenna aimed at efficient generation of the enantiomeric excess

during the chiral phototransformation at the nanoscale is to maximize  $\frac{g}{g_{\text{CPL}}}$  [31]. To achieve this, and in light of Eq. (2), certain conditions need to be satisfied, such as the spectral and spatial overlap of the electric and magnetic fields, while having  $\pi/2$  phase difference between them [28, 29, 32]. Several examples of metasurfaces realize these conditions using plasmon nanoantennas. The group of Chanda [33] provided a nanohole-nanodisk metasurface supporting two degenerate localized surface plasmon electric and magnetic modes. Here, the electromagnetic cavity mode, formed by the nanodisk at the bottom of the nanohole and the metallic nanohole rims, delivers a strongly chiral near-field that is designed to spectrally overlap with a C-H vibrational mode of a chiral molecule (camphor), experimentally improving its detection sensitivity by four orders of magnitude. The group of Gan [34] predicted a 1300-fold CD enhancement in a

metal-dielectric-metal metasurface when a chiral molecular interlayer is placed in the gap between the nanostructures. Other works have proposed Ag (Figure 3A) and Au plasmonic nanoapertures for the same purpose [35, 32]. We envision that producing superchiral fields by plasmon nanoantennas will not only provide the means for the extremely efficient handedness-dependent separation and detection of the chiral species, but will also aid in their enantiomeric resolution upon the initial chiral (photo)transformation.

The use of high-refractive-index semiconductor and dielectric nanoantennas presents the advantage of having strong electric and magnetic dipoles within the same nanostructure with the added benefit of low losses and high resonator quality factors. Such nanoantennas have been proposed by the group of Dionne for the generation of the chiral near-fields [7] (Figure 3C). An intriguing property of such high-index nanoantennas is the occurrence of

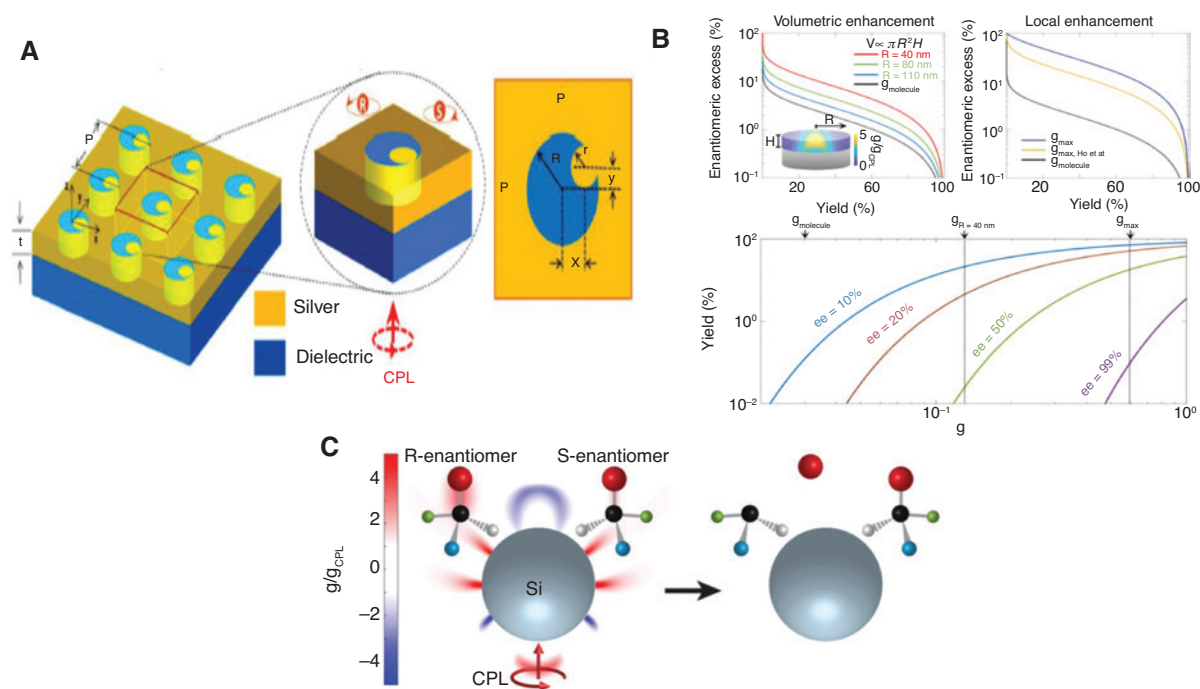


**Figure 3:** Several examples of theoretically proposed nanostructures showing superchiral fields suggested for enantiomeric separation. (A) Schematic representation of the plasmonic device formed by a periodic array of asymmetric nanoapertures for enantioselective optical process. Asymmetry parameters  $x$  and  $y$  in the right inset are employed to intensify the electromagnetic fields and introduce chiral asymmetry, respectively. Reproduced with permission from [35] © The Optical Society. (B) (upper left panel) Enantiomeric excess plotted against percent yield in a photoionization reaction based on thiocamphor molecule ( $g_{\text{molecule}} = 0.04$ ) for three different volume regions (different  $R$ ) above a GaP disk with fixed height ( $H = 40$  nm); (upper right panel) Enantiomeric excess plotted against percent yield in a photoionization reaction based on thiocamphor for no enhancement, the maximum point enhancement for a silicon sphere see [7], and that for the GaP disk metasurface (7- and 15-fold, respectively); (lower panel) percent yield plotted against absolute  $g$  for enantiomeric excesses (ee) of 10%, 20%, and 50%. Reprinted with permission from [30]. Copyright 2019 American Chemical Society. (C) Schematics for photolysis of a molecule near a silicon nanosphere illuminated by circularly polarized light. Enhanced preferential absorption near the nanosphere excites a vibrational mode in the right-handed ( $R$ ) enantiomer, leading to the dissociation of one bond while leaving the left-handed ( $S$ ) enantiomer intact. Reprinted with permission from [7]. Copyright 2017 American Chemical Society.

the so-called generalized Kerker condition, where higher order modes interfere constructively; specifically, the in-phase electric and magnetic modes spatially and spectrally overlap to produce highly directional forward light scattering [36, 37]. This effect has been proposed for the generation of enantiomeric excess by the near-field of the semiconductor nanostructures [29]. Calculations made by the group of Dionne [30] unearthed that a metasurface made of GaP nanodisks (see left inset in Figure 3B) could potentially have photoconversion reaction yields (i.e. the amount of substance that is being changed in an equilibrium reaction) for a thiocamphor up to 30% with an enantiomeric excess of 10%, as compared to the asymmetric reaction yield of 0.66% using just CP light. This is achieved by the 4.2-fold increase of the intrinsic molecular dissymmetry factor when the molecules are above the surface of a nanodisk (Figure 3B). Looking at the lower and the right inset of Figure 3B, it becomes apparent that, in order to achieve high reaction yields in the photodecomposition reaction while getting also a high value of enantiomeric excess, it is necessary to have a high value of  $g$  enhancement.

Fano-type resonances that typically result from the interaction of a high-quality (optical) resonator with a spectrally broader background (alternatively – lower order resonances) have been proposed for enantioselective trapping by using the high-intensity electromagnetic near-field. Specifically, using dipole-octupole Fano-type resonances, a transverse optical force appears, and optomechanical chiral sorting by trapping of sub-10 nm chiral particles becomes possible [38, 39]. Also using optical forces, the use of propagating surface plasmon polaritons (SPPs) has

been reported for enantioselective trapping [40]. The chirality of the medium is present through the index of refraction for right (+) and left (-) CPL as  $n_{\pm} = \sqrt{\epsilon_c \mu_c} \pm \kappa$ ;  $\kappa = \xi \mu_0 c_0$ , where  $\epsilon_c$ ,  $\mu_c$ , and  $\xi$  are the relative permittivity, permeability, and chirality of the medium, respectively, while  $\mu_0$  is the permeability of free space and  $c$  the speed of light. The presence of a chiral medium (in contact with the metal layer in the Kretschmann configuration) generates SPPs with handedness-dependent lateral optical forces in the evanescent field that act in opposite directions on an embedded chiral particle in the medium. Other conceptual works use the quantum spin Hall effect [41, 42] and similarly employ the evanescent optical fields, where chiral particles with different handedness experience opposite lateral forces also realizable at a metal-dielectric (chiral) interface [43]. A similar example proposed by the group of Qiu uses an interference field formed by two plane waves, where the state of polarization of the waves determines the lateral forces exerted on a chiral particle [44]. Optical tweezers are used as a very accurate enantioselection tool for the chiral nanoparticles, where optical trapping is dependent on the nanoparticles' structural chirality. The group of Dionne [45, 59, 60] recently demonstrated that plasmonic optical enantioselective trapping with a metallic tip could be achieved at 20 nm distance from the tip (see Figure 4). The same group introduced a technique to potentially separate enantiomers using a chiral atomic force microscope probe coupled to a plasmonic optical tweezer that exerts attractive or repulsive lateral forces, depending on the handedness of the employed CP light, with the difference in force of up to 10 pN [46].

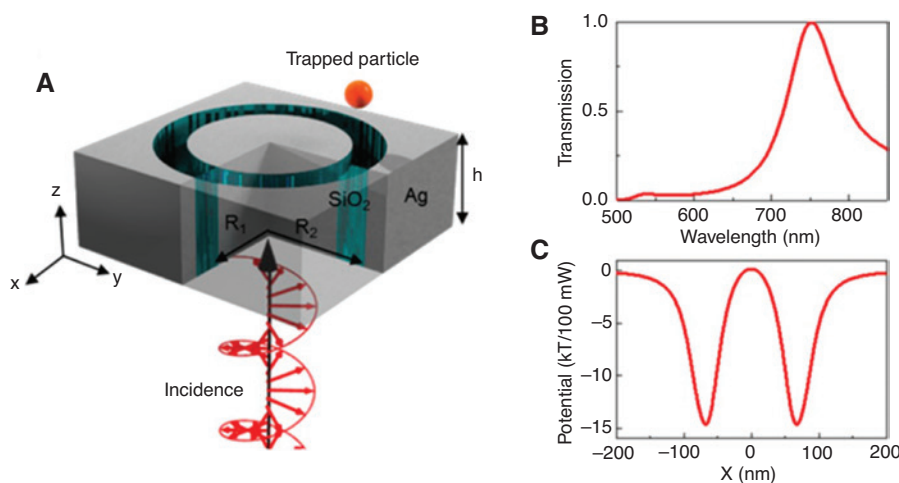


**Figure 4:** Optically trapping chiral particles.

(A) Schematic view of the plasmonic coaxial aperture. The incident light is left-handed circularly polarized and propagates along the +z direction. (B) and (C) are the calculated transmission and the one-dimensional trapping potential on an achiral particle with a refractive index of 1.45 and a diameter of 20 nm in water, 20 nm above the aperture. The trapping potential is normalized to 100 mW transmitted power. Adapted with permission from Ref. [45]. Copyright 2016 American Chemical Society.

It is highly intriguing to further explore the coupling of the molecular resonances to the electromagnetic superchiral cavities, mentioned above, as the means of achieving a substantial enhancement of detection of the chiral molecular species. We may ask ourselves whether further increasing the coupling strength in such system can favor the actual enantioseparation or even promote the enantiomeric excess of the optical near-field-controlled asymmetric photochemistry. A seminal paper by the group of Ebbesen [47] demonstrated the sizeable modification (specifically, slowing down) of the chemical reaction rate of a phototransformation when run under conditions of the so-called strong coupling of the molecular excitons and the optical mode of a Fabry-Perot cavity. Further perspective on the

chemistry involving strong coupling (the so-called polaritonic chemistry) is given in [48]. Indeed, as already pointed out in [33], the dissymmetry factor can increase when the cavity is tuned to the vibrational band of a chiral molecule. Although this is a surface-based enhancement phenomenon, the principle of using superchirality (as described in [7]) to rate-selectively photodecompose or in other way phototransform one enantiomer in the mix may become available. Here the strong coupling of the vibrational and/or optical molecular modes to the vibrational and/or optical superchiral modes of a meticulously designed electromagnetic cavity or nanoantenna would be essential.

It is also stimulating to explore the potential connection between chiral selectivity and another phenomenon

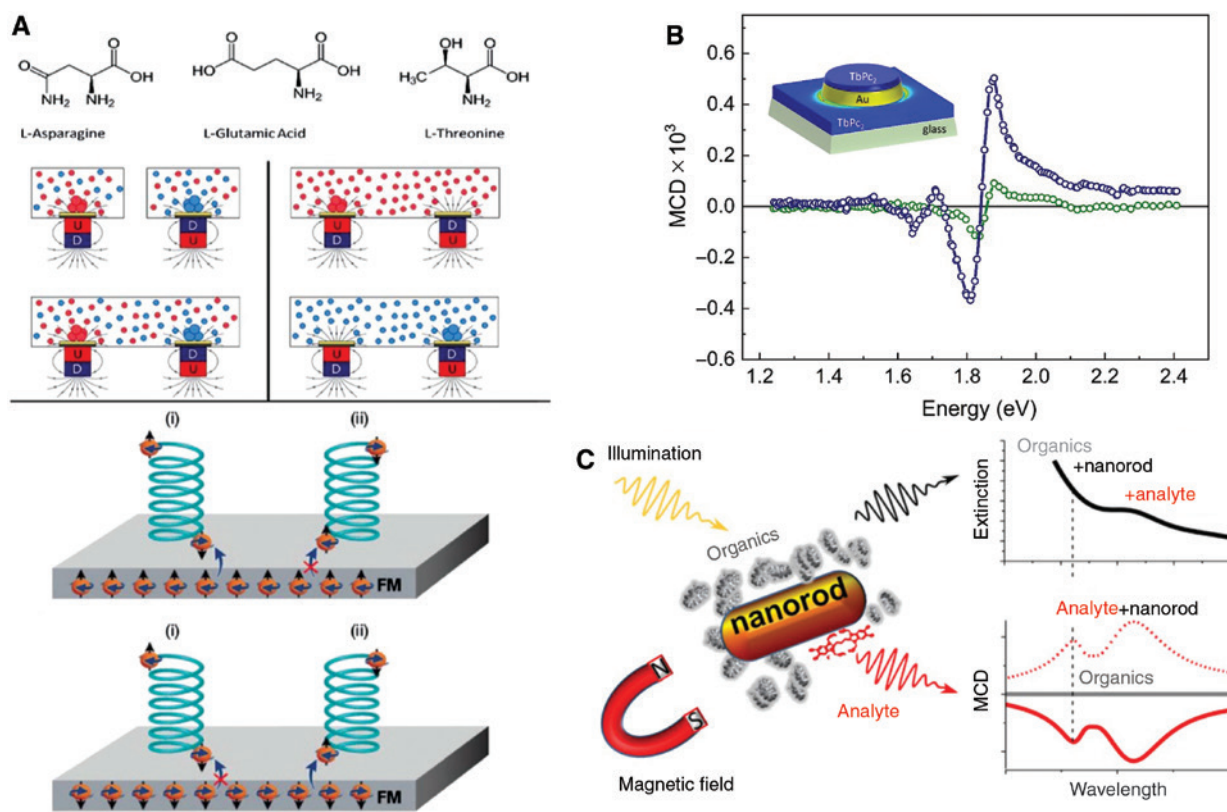


**Figure 5:** Using magnetic fields for enantiomeric separation, magneto-optical enhancement and sensing.

(A) Enantioselective deposition on a Si/Ni/Au ferromagnetic substrate of three different aminoacids. Depending of the orientation of the magnet underneath, it has been observed the chirally-preferential deposition of one handedness over its opposite in racemic mixtures (left inset) and enantiopure solutions (right inset). In the bottom inset, the suggested mechanism for the enantioselective crystallization. Charge polarization occurs when a chiral molecule approaches the ferromagnetic surface, accompanied by spin polarization. If the spins of the ferromagnet are aligned antiparallel to the spin of the chiral molecule, the interaction is stronger, increasing the probability of crystallization. Adapted from [50] – Published by The Royal Society of Chemistry. (B) Molecular part of the MCD spectrum (reported in differential extinction units vs photon energy) of TbPc2@Au corrected for the nanoantenna contribution (blue) and compared with the control MCD spectrum of TbPc2 (green) (inset: schematic representation of the TbPc2 layer on gold nanoantennas overlaid with finite difference time-domain (FDTD) simulations of the electromagnetic near-field). Adapted from [51] by permission of The Royal Society of Chemistry. (C) Schematic of an enhanced magneto-optical activity experiment in the strong coupling regime: the non-magnetic organic analyte (J-aggregates: extinction peak indicated by the black dashed line), binding to a plasmonic nanorod shows sizeable MCD (dashed and full lines in the MCD spectra represent the opposite directions of the magnetic field), while no MCD signal can be detected for the free-standing analyte (gray trace). Source: Ref. [58].

– magnetism. The latter is intimately connected with the molecular chiral phenomenon. In 2018, the Naaman group [49] demonstrated the selective absorption of the chiral molecules in a racemic mixture using magnetized achiral substrates, proposed to be driven by chirality-induced spin selectivity (CISS) effect. In a very recent experiment for the same group, three different aminoacids were crystalized in a ferromagnetic substrate, generating pure enantiomeric crystals (see Figure 5A). Depending of the direction of the magnet, one handedness is deposited in the substrate, while the other still remains in the solution [50]. An interesting first step of merging the magnetism at the molecular scale and optical nanoantennas was proposed in the recent work published by the group of Sessoli [51]. It demonstrates an enhancement in the magneto-optical activity of  $\text{TbPc}_2$ , a model single-molecule magnet (SMM), when combined with a simple plasmon antenna (Au nanodisks) (inset of Figure 5B). It has been demonstrated that plasmon antennas can be used conveniently for boosting magneto-optics in a variety of configurations [52–55]. In the aforementioned work, the plasmon antenna resonance spectrally overlaps with the excitonic absorption of the  $\text{TbPc}_2$ , which results in a fivefold increase in plasmon-enhanced molecular absorption (measured by magnetic circular dichroism, MCD) and similarly enhanced magneto-optical activity of the SMM (Figure 5B).

In this framework, the MCD signal resulting from the hybrid system can be treated as a linear superposition (i.e. weak coupling) of the magneto-optical signal from  $\text{TbPc}_2$  and a relatively strong contribution from the plasmon antenna. The latter, despite being diamagnetic, exhibits a sizeable magneto-optical activity arising from the perturbation induced by the applied magnetic field on the oscillation of charge carriers involved in plasmon resonance [56, 57]. Since this effect is qualitatively and quantitatively well understood, it becomes possible to model and subtract the plasmon contribution to the MCD signal, thus obtaining the plasmon-enhanced magneto-optical signature of SMMs. Interestingly, using the different magnetic behavior of the molecules (saturating their magnetization by increasing the applied magnetic field) and of the nanoantennas (linear to the applied magnetic field), it is possible to discriminate the nature of the MCD signal in different portions of the spectrum. Recently, the group of Liz-Marzan reported magneto-optical experiments on a Au nanorod antenna-dye assembly exhibiting strong coupling [58]. The authors found that the (non-magnetic) dye molecule, characterized by negligible magneto-optical activity in its native form, starts displaying a sizeable MCD spectral contribution when adsorbed on the Au nanorod antennas (Figure 5C). This effect has been ascribed to

the partial hybridization of the molecular optical resonance with that of the nanorod (which is MCD active, as described above). This example demonstrates a convincing strategy of transferring the properties while in the strong coupling regime, which might potentially include electromagnetic chiral interactions.

Looking forward, it is exciting to anticipate how exploring the various molecule-cavity coupling regimes, including the strong coupling with its marked emergence of the hybrid molecular states that allows bypassing the expected chemical reaction routes, and the intriguing connection between molecular chirality and magnetism, might eventually contribute to the development of unforeseen avenues towards highly efficient chiral chemistry at the nanoscale.

**Acknowledgments:** AD and EPV acknowledge the Knut and Alice Wallenberg Foundation for the project “Harnessing light and spins through plasmons at the nanoscale” (2015.0060, Funder Id: <http://dx.doi.org/10.13039/501100004063>). This work was furthermore supported by the European Union’s Horizon2020 Research and Innovation program, Grant agreement No. 737709 (FEMTOTERABYTE), Funder Id: <http://dx.doi.org/10.13039/501100000780>. EPV acknowledges the Swedish Energy Agency (Energimyndigheten), project P42028-1, Funder Id: <http://dx.doi.org/10.13039/501100004527>.

## References

- [1] Kartouzian A. Spectroscopy for model heterogeneous asymmetric catalysis. *Chirality* 2019;31:641–57.
- [2] Hentschel M, Schäferling M, Duan X, Giessen H, Liu N. Chiral plasmonics. *Sci Adv* 2017;3:e1602735.
- [3] Zhang Q, Hernandez T, Smith KW, et al. Unraveling the origin of chirality from plasmonic nanoparticle-protein complexes. *Science* 2019;365:1475–8.
- [4] Valev VK, Baumberg JJ, Sibilica C, Verbiest T. Chirality and chiroptical effects in plasmonic nanostructures: fundamentals, recent progress, and outlook. *Adv Mater* 2013;25:2517–34.
- [5] Feringa BL, van Delden RA. Absolute asymmetric synthesis: the origin, control, and amplification of chirality. *Angew Chem Int Ed* 1999;38:3418–38.
- [6] Zhdanov DV, Zadkov VN. Absolute asymmetric synthesis from an isotropic racemic mixture of chiral molecules with the help of their laser orientation-dependent selection. *J Chem Phys* 2007;127:244312–27.
- [7] Ho CS, Garcia-Etxarri A, Zhao Y, Dionne J. Enhancing enantioselective absorption using dielectric nanospheres. *ACS Photon* 2017;4:197–203.
- [8] Rijeesh K, Hashim PK, Noro S, Tamaoki N. Dynamic induction of enantiomeric excess from a prochiral azobenzene dimer under circularly polarized light. *Chem Sci* 2015;6:973–80.

- [9] Kim J, Lee J, Kim WY, et al. Induction and control of supramolecular chirality by light in self-assembled helical nanostructures. *Nat Commun* 2015;6:7959.
- [10] Hashim PK, Tamaoki N. Enantioselective photochromism under circularly polarized light. *ChemPhotoChem* 2019;3:347–55.
- [11] Kawasaki T, Sato M, Ishiguro S, et al. Enantioselective synthesis of near enantiopure compound by asymmetric autocatalysis triggered by asymmetric photolysis with circularly polarized light. *J Am Chem Soc* 2005;127:3274–5.
- [12] Noorduyn WL, Bode AA, van der Meijden M, et al. Complete chiral symmetry breaking of an amino acid derivative directed by circularly polarized light. *Nat Chem* 2009;1:729–32.
- [13] Fletcher SP. Growing the seeds of homochirality. *Nat Chem* 2009;1:692–3.
- [14] Tkachenko G, Brasselet E. Optofluidic sorting of material chirality by chiral light. *Nat Commun* 2014;5:3577.
- [15] Kravets N, Aleksanyan A, Chraïbi H, Leng J, Brasselet E. Optical enantioseparation of racemic emulsions of chiral microparticles. *Phys Rev Appl* 2019;11:044025.
- [16] Spesyvtseva SES, Shoji S, Kawata S. Chirality-selective optical scattering force on single-walled carbon nanotubes. *Phys Rev Appl* 2015;3:044003.
- [17] Tkachenko G, Brasselet E. Spin controlled optical radiation pressure. *Phys Rev Lett* 2013;111:033605.
- [18] Donato MG, Hernandez J, Mazzulla A, et al. Polarization-dependent optomechanics mediated by chiral microresonators. *Nat Commun* 2014;5:3656.
- [19] Tkachenko G, Brasselet E. Helicity-dependent three-dimensional optical trapping of chiral microparticles. *Nat Commun* 2014;5:4491.
- [20] Hernández RJ, Mazzulla A, Pane A, Volke-Sepúlveda K, Cipparrone G. Attractive-repulsive dynamics on light-responsive chiral microparticles induced by polarized tweezers. *Lab Chip* 2013;13:459–67.
- [21] Kravets N, Aleksanyan A, Brasselet E. Chiral optical Stern-Gerlach newtonian experiment. *Phys Rev Lett* 2019;122:024301.
- [22] Seo SH, Kim S, Han MS. Gold nanoparticle-based colorimetric chiral discrimination of histidine: application to determining the enantiomeric excess of histidine. *Anal Methods* 2014;6:73–6.
- [23] Zhang L, Xu C, Liu C, Li B. Visual chiral recognition of tryptophan enantiomers using unmodified gold nanoparticles as colorimetric probes. *Anal Chim Acta* 2014;809:123–7.
- [24] Zhang M, Ye BC. Colorimetric chiral recognition of enantiomers using the nucleotide-capped silver nanoparticles. *Anal Chem* 2011;83:1504–9.
- [25] Sun Y, Zhang L, Li H. Chiral colorimetric recognition of amino acids based on silver nanoparticle clusters. *New J Chem* 2012;36:1442–4.
- [26] Liu C, Li B, Xu C. Colorimetric chiral discrimination and determination of enantiomeric excess of D/L-tryptophan using silver nanoparticles. *Microchim Acta* 2014;181:1407–13.
- [27] Gogoi A, Mazumder N, Konwer S, Ranawat H, Chen NT, Zhuo GY. Enantiomeric recognition and separation by chiral nanoparticles. *Molecules* 2019;24:1007.
- [28] Schäferling M, Yin X, Giessen H. Formation of chiral fields in a symmetric environment. *Opt Express* 2012;20:26326–36.
- [29] Mohammadi E, Tavakoli A, Dehkoda P, et al. Accessible superchiral near-fields driven by tailored electric and magnetic resonances in all-dielectric nanostructures. *ACS Photon* 2019;6:1939–46.
- [30] Solomon ML, Hu J, Lawrence M, García-Etxarri A, Dionne JA. Enantiospecific optical enhancement of chiral sensing and separation with dielectric metasurfaces. *ACS Photon* 2019;6:43–9.
- [31] Tang Y, Cohen AE. Optical chirality and its interaction with matter. *Phys Rev Lett* 2010;104:163901.
- [32] Hendry E, Mikhaylovskiy RV, Barron LD, Kadodwala M, Davis TJ. Chiral electromagnetic fields generated by arrays of nanoslits. *Nano Lett* 2012;12:3640–4.
- [33] Vázquez-Guardado A, Chanda D. Superchiral light generation on degenerate achiral surfaces. *Phys Rev Lett* 2018;120:137601.
- [34] Rui G, Hu H, Singer M, Jen YJ, Zhan Q, Gan Q. Symmetric meta-absorber-induced superchirality. *Adv Opt Mater* 2019;7:1901038.
- [35] Champi HAA, Bustamante RH, Salcedo WJ. Optical enantioseparation of chiral molecules using asymmetric plasmonic nanoapertures. *Opt Mater Express* 2019;9:1763–75. <https://doi.org/10.1364/OME.9.001763>.
- [36] Kerker M, Wang DS, Giles CL. Electromagnetic scattering by magnetic spheres. *J Opt Soc Am* 1983;73:765–7.
- [37] Liu W, Kivshar YS. Generalized Kerker effects in nanophotonics and meta-optics. *Opt Express* 2018;26:13085–105.
- [38] Cao T, Mao L, Qiu Y, et al. Fano resonance in asymmetric plasmonic nanostructure: separation of sub-10 nm enantiomers. *Adv Opt Mater* 2019;7:1801172.
- [39] Cao T, Qiu Y. Lateral sorting of chiral nanoparticles using Fano-enhanced chiral force in visible region. *Nanoscale* 2018;10:566–74.
- [40] Zhang Q, Li J, Liu X. Optical lateral forces and torques induced by chiral surface-plasmon-polaritons and their potential applications in recognition and separation of chiral enantiomers. *Phys Chem Chem Phys* 2019;21:1308–14.
- [41] Bliokh KY, Smirnova D, Nori F. Quantum spin Hall effect of light. *Science* 2015;348:1448–51.
- [42] Bliokh KY, Nori F. Transverse and longitudinal angular momenta of light. *Phys Rep* 2015;592:1–38.
- [43] Zhang Q, Li J, Liu X, Gelmecha DJ, Zhang W. Optical screwdriving induced by the quantum spin Hall effect of surface plasmons near an interface between strongly chiral material and air. *Phys Rev A* 2018;97:013822.
- [44] Zhang T, Mahdy MRC, Liu Y, et al. All-optical chirality-sensitive sorting via reversible lateral forces in interference fields. *ACS Nano* 2017;11:4292–300.
- [45] Zhao Y, Saleh AAE, Dionne JA. Enantioselective optical trapping of chiral nanoparticles with plasmonic tweezers. *ACS Photon* 2016;3:304–9.
- [46] Zhao Y, Saleh AAE, van de Haar MA, et al. Nanoscopic control and quantification of enantioselective optical forces. *Nat Nanotechnol* 2017;12:1055–9.
- [47] Hutchison JA, Schwartz T, Genet C, Devaux E, Ebbesen TW. Modifying chemical landscapes by coupling to vacuum field. *Angew Chem Int Ed* 2012;51:1592–6.
- [48] Hertzog M, Wang M, Mony J, Börjesson K. Strong light–matter interactions: a new direction within chemistry. *Chem Soc Rev* 2019;48:937–61.
- [49] Banerjee-Ghosh K, Dor OB, Tassinari F, et al. Separation of enantiomers by their enantiospecific interaction with achiral magnetic substrates. *Science* 2018;360:1331–4.



- [50] Tassinari F, Steidel J, Paltiel S, et al. Enantioseparation by crystallization using magnetic substrates. *Chem Sci* 2019;10:5246–50.
- [51] Pineider F, Pedrueza-Villalmanzo E, Serri M, et al. Plasmon-enhanced magneto-optical detection of single-molecule magnets. *Mater Horiz* 2019;6:1148–55.
- [52] Zubritskaya I, Maccaferri N, Ezeiza XI, Vavassori P, Dmitriev A. Magnetic control of the chiroptical plasmonic surfaces. *Nano Lett* 2018;18:302–7.
- [53] Zubritskaya I, Lodewijks K, Maccaferri N, et al. Active magneto-plasmonic ruler. *Nano Lett* 2015;15:3204–11.
- [54] Lodewijks K, Maccaferri N, Pakizeh T, et al. Magnetoplasmonic design rules for active magneto-optics. *Nano Lett* 2014;14:7207–14.
- [55] Armelles G, Cebollada A, García-Martín A, González MU. Magnetoplasmonics: combining magnetic and plasmonic functionalities. *Adv Opt Mater* 2013;1:10–35.
- [56] Sepulveda B, Gonzalez-Diaz JB, Garcia-Martín A, Lechuga LM, Armelles G. Plasmon-induced magneto-optical activity in nanosized gold disks. *Phys Rev Lett* 2010;104:147401.
- [57] Pineider F, Campo G, Bonanni V, et al. Circular magnetoplasmonic modes in gold nanoparticles. *Nano Lett* 2013;13:4785–9.
- [58] Melnikau D, Govyadinov AA, Sanchez-Iglesias A, Grzelczak M, Liz-Marzan LM, Rakovich YP. Strong magneto-optical response of nonmagnetic organic materials coupled to plasmonic nanostructures. *Nano Lett* 2017;17:1808–13.
- [59] Schäferling M, Giessen H. Comment on “Enantioselective Optical Trapping of Chiral Nanoparticles with Plasmonic Tweezers”. *ACS Photon* 2018;5:2533–4.
- [60] Zhao Y, Dionne J. Response to “comment on ‘Enantioselective Optical Trapping of Chiral Nanoparticles with Plasmonic Tweezers’”. *ACS Photon* 2018;5:2535–6.